

7-19-2023

Effects of cut depth and cut spacing on a conical pick in rock cutting

Jiu-bo LIAO

School of Resources and Safety Engineering, Central South University, Changsha, Hunan 410083, China

Xi-bing LI

School of Resources and Safety Engineering, Central South University, Changsha, Hunan 410083, China

Shao-feng WANG

School of Resources and Safety Engineering, Central South University, Changsha, Hunan 410083, China

Kun DU

School of Resources and Safety Engineering, Central South University, Changsha, Hunan 410083, China

Follow this and additional works at: <https://rocksoilmech.researchcommons.org/journal>



Part of the [Geotechnical Engineering Commons](#)

Recommended Citation

LIAO, Jiu-bo; LI, Xi-bing; WANG, Shao-feng; and DU, Kun (2023) "Effects of cut depth and cut spacing on a conical pick in rock cutting," *Rock and Soil Mechanics*: Vol. 44: Iss. 4, Article 3.

DOI: 10.16285/j.rsm.2022.6667

Available at: <https://rocksoilmech.researchcommons.org/journal/vol44/iss4/3>

This Article is brought to you for free and open access by Rock and Soil Mechanics. It has been accepted for inclusion in Rock and Soil Mechanics by an authorized editor of Rock and Soil Mechanics.

Effects of cut depth and cut spacing on a conical pick in rock cutting

LIAO Jiu-bo, LI Xi-bing, WANG Shao-feng, DU Kun

School of Resources and Safety Engineering, Central South University, Changsha, Hunan 410083, China

Abstract: In order to study the effects of different cut depths and cut spacings on cutting force and specific cutting energy acting on a conical pick, the laboratory linear rock cutting tests were carried out on carbonaceous slate and rhyolite elastic rock based on the TRW-300 true triaxial electro-hydraulic servo system and self-designed innovative pick loading platform. Experimental results indicate that there were four types of failure modes on a conical pick in rock cutting, and there was a synergistic effect between two adjacent picks. The mean cutting force linearly increases with the increasing cut depth and cut spacing. The specific cutting energy decreases with the increasing cut depth in a power-function way. The specific cutting energy decreases first and then increases with the increasing ratio of cut spacing to cut depth, and there is a minimum value that is optimal, where it is far less than energy under an unrelieved cutting groove. The optimum value of the ratio of cut spacing to cut depth is 2 or 3. Based on the results of laboratory tests, the pick arrangement on the cutting head of the cantilever roadheader is optimized, and applied to the field industrial test of non-explosive tunneling of roadheader, which significantly increases tunneling efficiency and reduces tunneling costs.

Keywords: conical pick; rock cutting; cut depth; cut spacing; specific cutting energy

1 Introduction

Currently, conventional drilling and blasting methods are widely used in underground engineering projects such as tunnel and mine excavation. However, compared to drilling and blasting method, non-explosive mechanized cutting has many advantages, such as better tunnel-section forming quality, controllable overbreak/underbreak, less damage to surrounding rocks, better safety conditions, higher excavation efficiency, lower excavation costs, and higher degree of mechanization and intelligence. Therefore, it has been widely applied in the excavation of soft rocks. However, hard rocks are characterized by high hardness, high strength, good integrity and strong abrasiveness, which makes picks easy to wear when breaking rocks, shortening their life and increasing the time required for repair and replacement, thus leading to low excavation efficiency and high excavation costs. In addition to improving the wear resistance of picks materials, in-depth research on the rock-breaking mechanism by picks, and the optimization design of cutting parameters and the arrangement of picks on the cutting head is the main method for improving the cutting ability of picks for rock breaking and reducing their consumption^[1–8]. To improve rock-breaking efficiency and cutting performance, many scholars have studied the effects of rock properties, geometric parameters of picks and cutting parameters on rock-breaking behavior. This provides a basis for optimizing design and selection of rock-breaking machinery^[9–14].

Balci et al.^[15] conducted comprehensive rock-cutting tests on 23 different samples of rocks, minerals and ores to obtain their optimal specific cutting energy. They used statistical methods to analyze the relationship between optimal specific cutting energy and rock mechanical properties. Tiryaki et al.^[16] associated rock properties with specific cutting energy by using bivariate correlation analysis and linear regression analysis to evaluate their relationship. Wang et al.^[17] used conical picks to conduct indentation tests on cuboid rocks, studied the effect of uniaxial lateral stress on rock cuttability, established a theoretical model and analyzed specific energy consumption and its related factors. Zhang et al.^[18] analyzed the energy requirements for rock fragmentation in laboratory tests and engineering operations, and discussed the effects of loading rate, confining pressure, prefabricated cracks, wear and thermal energy on specific fracture energy of rocks. Wang et al.^[19] established a cutting force prediction model for conical picks and discussed the effect of its geometric parameters on cutting force. Li et al.^[20] conducted rock-cutting tests and simulations, studied the effects of installation parameters and geometric shapes of picks on cutting performance, and proposed a multi-attribute index to evaluate cutting performance and select optimal cutting parameters. Liang et al.^[21] used linear fitting and power function fitting to describe statistical relationships between cutting force, normal force and cut depth. As the cut depth increases, the ratio of normal force to cutting force decreases linearly; as the cut spacing increases,

both cutting force and normal force increase linearly while their ratio decreases in a power function. Wang et al.^[22–25] used conical pick for rock indentation tests to study the relationship between rock cuttability and confining pressure conditions as well as rock strength.

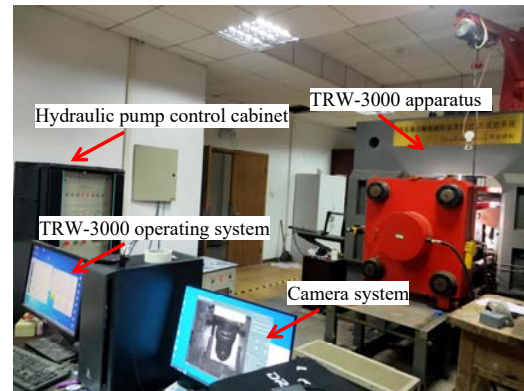
The aforementioned laboratory experimental research mainly focuses on studying the effects of rock properties, pick geometry parameters, confining pressure on cutting loads and specific cutting energy. However, there is still a lack of exploration into the effects of related cutting parameters such as cut depth, cut spacing, and the ratio of cut spacing to cut depth, on cutting force and specific cutting energy. The specific cutting energy of picks refers to the energy consumed by a unit volume of rocks during cutting. It is closely related to rock properties, pick geometry parameters, and cutting parameters. It is commonly used to evaluate rock cuttability and to measure the efficiency of roadheaders in cutting. Based on this, this paper uses a self-designed pick loading platform to conduct straight-line cutting tests on two types of rock samples: carbonaceous slate and rhyolite clastic rock. The study investigates the effects of different combinations of cut depth and cut spacing on cutting force and specific cutting energy. Relevant mathematical models are established, and conclusions are drawn from them to optimize the arrangement of picks in the cutting head of SCR260 roadheaders. This optimization method is applied in an industrial test at a non-explosive excavation site in a segmented roadway with a length of 3 870 meters at a silver-polymetallic mine in Sichuan Province.

2 Laboratory tests

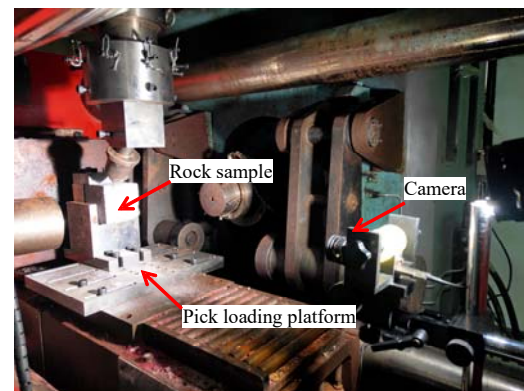
2.1 Test equipment and picks

The experimental equipment comes complete with TRW-3000 true triaxial electro-hydraulic servo testing system. The maximum static loading force of testing system in x , y , and z directions exceeds 2 000 kN for each direction. Real-time loading forces and displacements in each direction can be recorded through control system. The loading process is real-timely monitored by a camera system which captures images at a frequency of 60 frames per second. Figure 1 presents the testing system for indoor experiments. Figure 1(a) shows an overall view, and Fig. 1(b) shows the pick loading platform and camera.

This experimental study utilizes an innovative pick loading platform that is independently designed, which consists of a base, a sample table, a sleeve, and a pick base. The base of the platform is secured to the equipment base using four bolts in two horizontal directions. The sample table is fixed to the base using four bolts and can be moved forward and backward to significantly change



(a) Overall view of the testing system



(b) Pick loading platform and camera

Fig. 1 Indoor test system

the cut depth. Additionally, the cut depth of the sample can be finely adjusted by placing steel plates of varying thicknesses in the sample trough on the sample table. By shifting the installation position of the base on the horizontal plane left and right, different cut spacings can be achieved for cutting tests. The loading disk of the testing system is connected to the pick base through a sleeve, and the pick is fixed to the pick base using bolts. The pick angle can be changed by rotating the pick base. Figure 2 shows a schematic diagram of each part of the pick loading platform in these tests, while Fig. 3 displays a schematic diagram of a TBJJ.31S2 conical pick.

2.2 Physical and mechanical properties of rocks

For our indoor experiments, carbonaceous slate and rhyolite clastic rock were selected as cut objects. Rock samples were cut from intact rock blocks and made into complete rectangular samples with a size of 100 mm×100 mm×70 mm and each end surface was polished smooth. Before conducting cutting tests, physical and mechanical parameters such as uniaxial compressive strength, tensile strength, elastic modulus, Poisson's ratio, cohesion, and internal friction angle were tested for each type of rock specimen. The uniaxial compression test was conducted using Instron 1346 universal material testing machine produced by Instron Ltd., a British company (Fig. 4(a)). Six standard cylindrical specimens with dimensions of

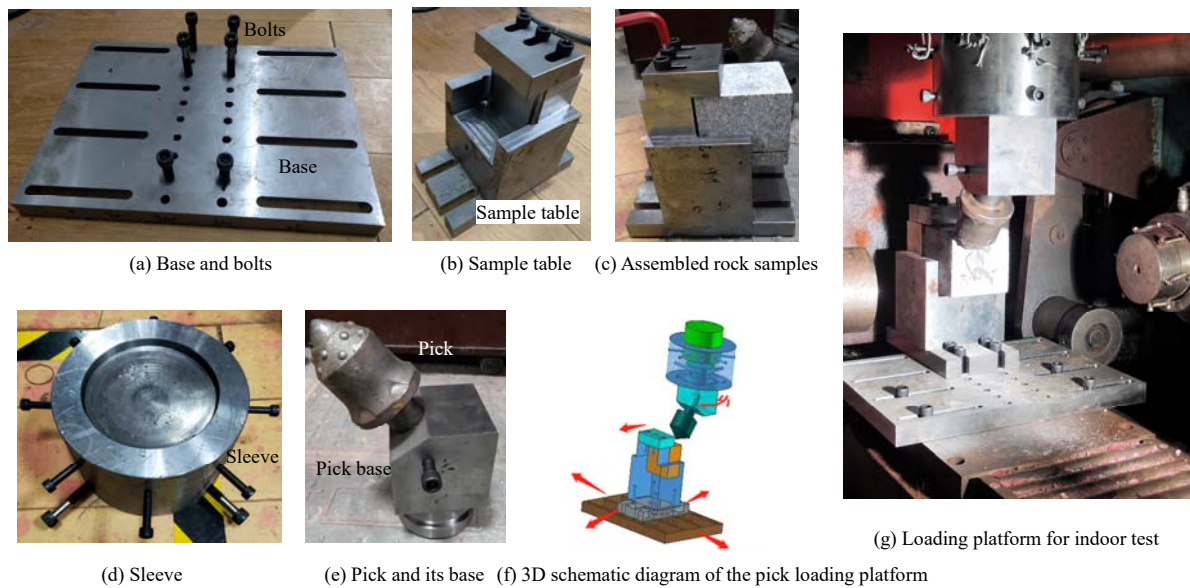
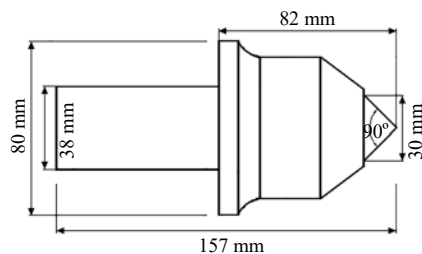


Fig. 2 Schematic diagram of pick loading platform



(a) Physical picture



(b) Size diagram

Fig. 3 Diagram of the dimensions of the conical pick

$\varnothing 50 \text{ mm} \times 100 \text{ mm}$ were prepared for each type of rock specimen for uniaxial compression tests, and an average

value from six tests was obtained. The tensile strength tests were conducted using an Instron 1342 low-cycle fatigue testing machine (Fig. 4(b)). Six circular specimens with dimensions of $\varnothing 50 \text{ mm} \times 25 \text{ mm}$ were prepared for each type of rock specimen for Brazilian tests, and an average value from six tests was also obtained. Cohesion and internal friction angle tests were conducted using an Instron 1346 universal material testing machine (Fig. 4(c)). Six standard cylindrical specimens with dimensions of $\varnothing 50 \text{ mm} \times 100 \text{ mm}$ were prepared for each type of rock specimen, and the final values were obtained by averaging six tests. Table 1 lists the physical and mechanical parameters of the rocks.

2.3 Experimental program and data processing

2.3.1 Experimental program

The rock specimen is fixed in the sample trough of the pick loading platform, and the cutting point position of the pick is controlled by changing the installation position of pick platform base and sample table, where the angle between the pick axis and the projection line of the contact

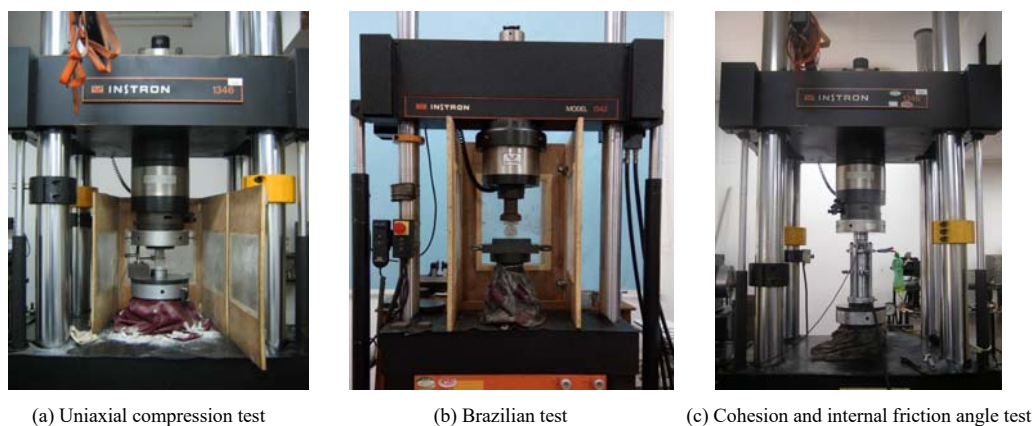
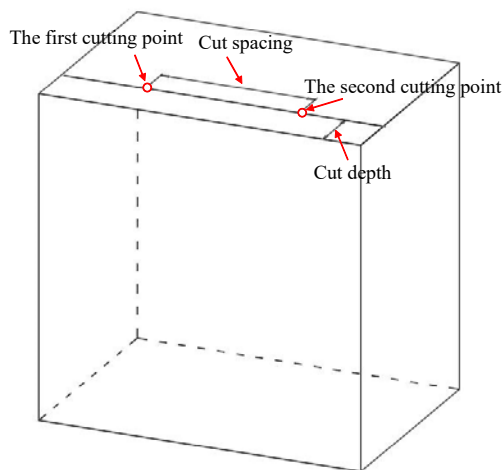


Fig. 4 Test diagrams of rock mechanical parameters

Table 1 Physical and mechanical parameters of rocks

Rock type	Density ($\text{g} \cdot \text{cm}^{-3}$)	Elastic modulus /GPa	Poisson's ratio	Uniaxial compressive strength /MPa	Tensile strength /MPa	Cohesion /MPa	Internal friction angle /($^{\circ}$)
Carbonaceous slate	2.76	46.39	0.20	55.26	2.11	13.84	44.83
Rhyolite clastic rock	2.77	42.28	0.25	79.78	3.60	16.71	46.09

surface of the specimen is 54° . Previous studies have shown that cutting speed has little effect on cutting force and specific cutting energy. The cutting speed in the z -direction is set at 0.5 mm/min . The experiments are divided into two cutting modes, with each specimen undergoing two cuts: one without groove and one with previous groove. When cut spacing is small, effective rock fragmentation can be achieved between grooves. The ratio of cut spacing to cut depth is a commonly used parameter for design and selection of rock-breaking machine. Bilgin et al.^[27] found that there exists an optimal value for this ratio that minimizes specific cutting energy based on experiments under a cut depth between 3 and 9 mm. For different types of rocks, this ratio ranges from 2 to 5. In our experiments, cut depths are set at 4, 8, 12, and 16 mm, while cut spacings are set at 1, 2, 3, and 4 times the cutting depth for each type of rock. There are a total of sixteen combinations for each type of rock, with three tests for each scenario to obtain an average value. Figure 5 shows a three-dimensional schematic diagram of the pick loading scheme. Cutting force, displacement and failure patterns are recorded synchronously during loading.

**Fig. 5 Three-dimensional schematic diagram of pick loading scheme**

2.3.2 Data processing

The relationship between cutting force and displacement of the specimen during loading is recorded. When large rock fragments are observed to be produced and the cutting force curve on the control panel rapidly decrease to zero, testing should stop immediately. The recorded cutting

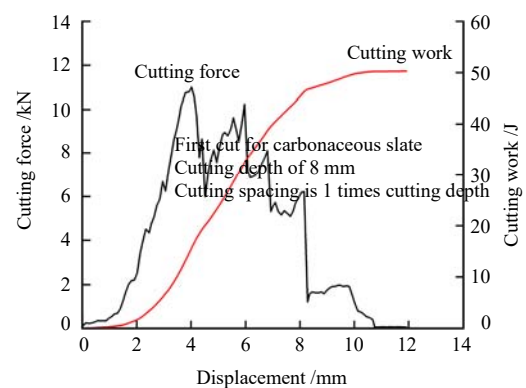
displacement at the moment when the cutting force just fall to zero is the maximum depth of pick penetration into the rock. The average cutting force within this range of cutting displacement is calculated using the following formula:

$$F_m = \frac{1}{n} \sum_{i=1}^n F_i \quad (1)$$

where F_m represents the average cutting force (kN); n represents the number of data; and F_i represents the cutting force (kN) of the i_{th} data.

The area enclosed by the cutting force curve and the X -axis before the maximum cutting displacement is integrated to calculate the cutting work W during the rock-breaking process by the pick. The relationship curves between cutting force, cutting work, and cutting displacement during the first cut of sample TB-8-1 are illustrated in Fig. 6. The cutting work during both the first cut (without groove) and second cut (with groove) of each sample is calculated separately. The rock fragments after both cuts are weighed, and finally, the specific cutting energy is calculated using the following formula:

$$E = \frac{\left(\int_0^{\Delta s} F ds \right) \cdot \rho}{m} \quad (2)$$

**Fig. 6 Cutting force and cutting work versus cutting displacement for the first cutting of specimen TB-8-1**

where E is specific cutting energy (J/cm^3), F is cutting force (kN), s is displacement (mm), ρ is density (g/cm^3), and m is mass (g).

2.4 Analysis of test results

Tables 2 and 3 provide detailed rock-breaking parameters of carbonaceous slate and rhyolite clastic rock during two cutting operations.

Table 2 Rock breaking parameters for indoor tests of carbonaceous slate

Specimen No.	Cutting depth /mm	Cutting spacing /mm	Ratio of cut spacing to cutting depth	Average cutting force for the first cut /kN	Average cutting force for the second cut /kN	Cutting work for the first cut /J	Cutting work for the second cut /J	Volume of fragments for the first cut /cm ³	Volume of fragments for the second cut /cm ³	Specific cutting energy for the first cut /(J • cm ⁻³)	Specific cutting energy for the second cut /(J • cm ⁻³)	Reduction of specific cutting energy /%
TB-4-1	4	4	1	2.67	1.84	27.39	16.60	16.58	16.05	1.652	1.034	37.41
TB-4-2	4	8	2	2.95	1.96	29.88	17.63	18.47	18.68	1.618	0.944	41.66
TB-4-3	4	12	3	2.74	2.05	31.14	19.02	19.15	19.61	1.626	0.970	40.34
TB-4-4	4	16	4	3.43	2.17	33.09	23.19	19.36	20.04	1.709	1.157	32.30
TB-8-1	8	8	1	4.71	2.14	52.19	35.96	34.89	37.54	1.496	0.958	35.96
TB-8-2	8	16	2	6.28	2.62	59.21	35.26	40.06	42.79	1.478	0.824	44.25
TB-8-3	8	24	3	5.79	3.37	52.09	34.35	35.58	44.67	1.464	0.769	47.47
TB-8-4	8	32	4	5.53	4.05	57.98	60.85	38.60	55.83	1.502	1.090	27.43
TB-12-1	12	12	1	7.12	2.84	77.84	59.13	57.66	70.81	1.350	0.835	38.15
TB-12-2	12	24	2	8.58	3.07	90.28	60.43	69.13	84.87	1.306	0.712	45.48
TB-12-3	12	36	3	9.27	3.58	92.62	57.28	69.22	82.18	1.338	0.697	47.91
TB-12-4	12	48	4	8.65	4.54	85.91	73.03	62.89	80.97	1.366	0.902	33.97
TB-16-1	16	16	1	8.86	4.98	89.69	75.44	70.73	96.23	1.268	0.784	38.17
TB-16-2	16	32	2	11.43	5.76	100.87	65.54	82.01	93.36	1.230	0.702	42.93
TB-16-3	16	48	3	10.82	6.54	97.41	72.74	78.43	97.25	1.242	0.748	39.77
TB-16-4	16	64	4	9.64	6.86	89.89	70.07	72.61	91.71	1.238	0.764	38.29

Table 3 Rock breaking parameters for indoor tests of rhyolitic clastic rock

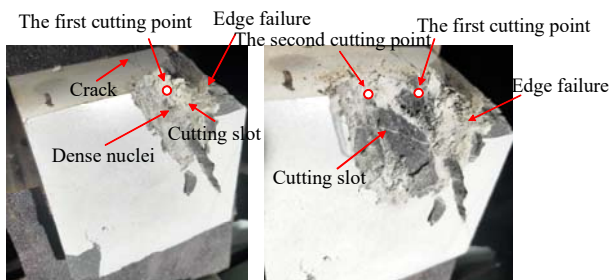
Specimen No.	Cutting depth /mm	Cutting spacing /mm	Ratio of cut spacing to cutting depth	Average cutting force for the first cut /kN	Average cutting force for the second cut /kN	Cutting work for the first cut /J	Cutting work for the second cut /J	Volume of fragments for the first cut /cm ³	Volume of fragments for the second cut /cm ³	Specific cutting energy for the first cut /(J • cm ⁻³)	Specific cutting energy for the second cut /(J • cm ⁻³)	Reduction of specific cutting energy /%
SX-4-1	4	4	1	4.65	2.57	43.45	35.20	10.69	12.83	4.065	2.743	32.52
SX-4-2	4	8	2	4.47	2.77	40.95	34.73	9.53	13.28	4.298	2.615	39.16
SX-4-3	4	12	3	3.86	2.86	44.58	40.20	10.82	14.72	4.121	2.731	33.73
SX-4-4	4	16	4	4.16	2.98	42.15	30.31	10.39	10.60	4.057	2.859	29.53
SX-8-1	8	8	1	7.62	3.54	79.17	71.60	22.68	29.43	3.490	2.433	30.29
SX-8-2	8	16	2	8.17	3.82	85.92	68.72	24.44	28.57	3.515	2.405	31.58
SX-8-3	8	24	3	8.37	3.98	71.07	60.94	20.41	27.94	3.482	2.181	37.36
SX-8-4	8	32	4	8.67	4.41	66.72	57.55	19.33	22.34	3.452	2.576	25.38
SX-12-1	12	12	1	9.24	3.81	105.21	83.32	35.47	45.76	2.966	1.821	38.60
SX-12-2	12	24	2	10.36	3.94	119.34	78.78	41.61	44.56	2.868	1.768	38.35
SX-12-3	12	36	3	11.01	4.17	110.50	72.06	37.79	44.93	2.924	1.604	45.14
SX-12-4	12	48	4	9.68	4.86	103.39	86.83	35.46	46.04	2.916	1.886	35.32
SX-16-1	16	16	1	13.55	5.36	120.54	117.76	44.45	69.03	2.712	1.706	37.09
SX-16-2	16	32	2	12.49	6.26	127.91	106.56	47.73	70.76	2.680	1.506	43.81
SX-16-3	16	48	3	13.25	6.96	128.20	105.52	47.06	72.37	2.724	1.458	46.48
SX-16-4	16	64	4	14.28	7.47	134.06	117.97	49.62	68.19	2.702	1.730	35.97

2.4.1 Failure modes

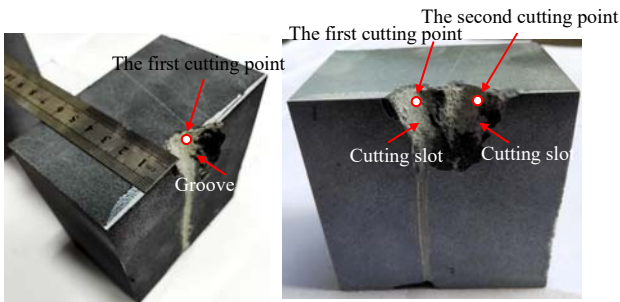
Typical failure modes of carbonaceous slate specimens are depicted in Fig. 7. According to Tables 2 and 3, as well as Fig. 7, as the intrusion of pick and the increase of cutting displacement, four modes of failure occur sequentially in the cutting process: elastic deformation, generation of small particle debris and dense nuclei, formation of cracks in various directions, and main crack propagation as well as collapse of large rock fragments. When the pick invades the rock, a complex stress field consisting of tensile, compressive and shear stress is generated due to the squeezing of the rock by the pick spherical surface.

The compressed rock undergoes severe plastic deformation and failure. Fine particle debris is formed in the initial crushing zone and aggregates into dense nuclei under extreme pressure. During testing, sharp sounds are emitted while smoke and dust are released simultaneously. The dense nuclei gradually accumulate energy and transfer cutting force and energy to surrounding rocks. When a certain stress in surrounding rocks exceeds its corresponding strength, a crack source is formed. Numerous cracks in various directions gradually expand and coalesce with each other, causing local small rock fragments to collapse. Mixed cracks extend along joints or bedding planes with

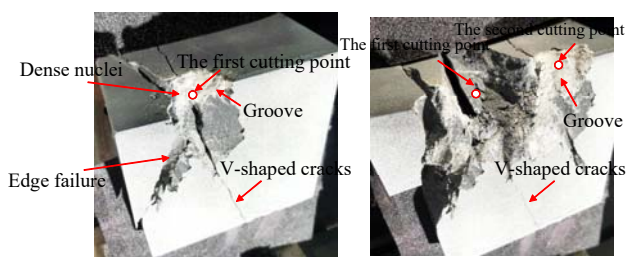
minimum energy in rocks. When the distance between cutting point and side free surface is relatively large compared to cutting depth, nearly two main V-shaped cracks that penetrate to free surfaces appear for almost all specimens. As cutting displacement increases, these cracks gradually extend downward inwardly until they finally cause large rock fragments to separate from their matrix. When the distance is relatively small, lateral cracks occur, leading to edge failure. A larger cutting depth results in more obvious main cracks and larger collapsed rock fragments. When rock fragments collapse, the cutting force drops rapidly from the peak, and a cut is completed.



(a) Cutting depth, cut spacing and their ratio are 16 mm, 16 mm and 1, respectively.



(b) Cutting depth, cut spacing and their ratio are 12 mm, 24 mm and 2, respectively.



(c) Cutting depth, cut spacing and their ratio are 16 mm, 48 mm and 3, respectively

Fig. 7 Typical failure diagram of carbonaceous slate specimens

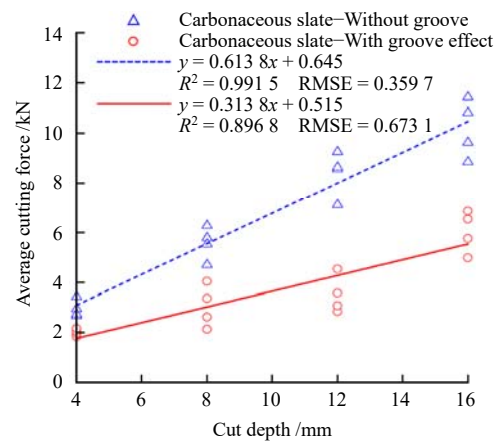
For a given cut depth, it is found during cutting experiments that if cut spacing is too small, as shown in Fig. 7(a), the rocks from two grooves are overly fragmented into finer debris and particles. Moreover, a large amount of dust is generated during cutting process, indicating that over-cutting occurs and cutting conditions are poor. Although

the cutting force is small, the specific cutting energy is relatively high. If cut spacing is moderate, as shown in Figs. 7(b) and 7(c), larger rock fragments collapse during cutting process, and there are many fragments remaining in a semi-peeling state between two successive cuts. This suggests that cracks formed between adjacent grooves can coalesce well and work synergistically to break the specimen, resulting in an optimal cutting condition. If cut spacing is too large, there is no interaction between adjacent grooves and obvious rock ridges exist between them. Cracks formed between two successive grooves cannot coalesce each other to generate effective avalanche, resulting in an under-cutting state with high specific cutting energy. Therefore, the effect of cut spacing on specific cutting energy is closely related to cut depth. The minimum specific cutting energy under different combinations results from joint effects of cut spacing and cut depth.

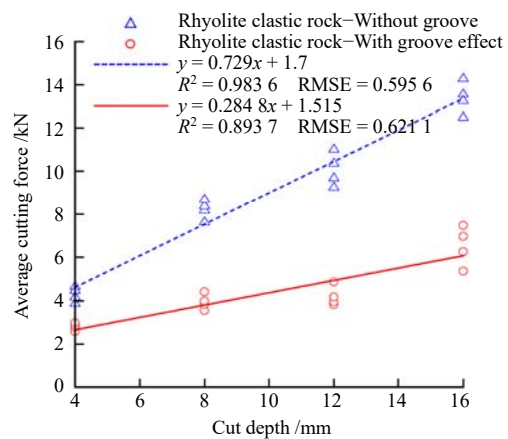
2.4.2 Cutting force

(1) Effect of cut depth on cutting force

Regression analysis was performed on the relationship between the average cutting force and cut depth for carbonaceous slate and rhyolite clastic rock, as shown in Fig. 8. It can be seen that as cut depth increases, both



(a) Carbonaceous slate



(b) Rhyolite clastic rock

Fig. 8 Diagrams of average cutting force versus cutting depth

types of rocks show an increasing trend in average cutting force with and without grooves. Under the same cutting parameters, the average cutting force of rhyolite clastic rock is generally greater than that of carbonaceous slate specimens. There is a strong linear relationship between the average cutting force without grooves and the cut depth, and the coefficient of determination R^2 and root mean square error (RMSE) are calculated to evaluate the rationality of the regression model using following formulas:

$$R^2 = 1 - \frac{\sum_{i=1}^m (y_{\text{test}}^{(i)} - \hat{y}_{\text{mod}}^{(i)})^2}{\sum_{i=1}^m (y_{\text{test}}^{(i)} - \bar{y}_{\text{test}}^{(i)})^2} \quad (3)$$

$$\text{RMSE} = \sqrt{\frac{1}{m} \sum_{i=1}^m (y_{\text{test}}^{(i)} - \hat{y}_{\text{mod}}^{(i)})^2} \quad (4)$$

where $y_{\text{test}}^{(i)}$, $\hat{y}_{\text{mod}}^{(i)}$, $\bar{y}_{\text{test}}^{(i)}$ and m are tested values, predicted values, average tested values and tested data number.

Without groove effects, the calculation results are $R^2 = 0.9915$ and $\text{RMSE} = 0.3597$ for carbonaceous slate specimens and $R^2 = 0.9836$ and $\text{RMSE} = 0.5956$ for rhyolite clastic rocks. A high coefficient of determination and a small root mean square error indicates that the established regression model has good rationality. The linear relationship between average cutting force with groove effects and cut depth is weak, with $R^2 = 0.8968$ and $\text{RMSE} = 0.6731$ for carbonaceous slate specimens and $R^2 = 0.8937$ and $\text{RMSE} = 0.6211$ for rhyolite clastic rocks, which indicates that rock fragments falling between grooves have a significant effect on cutting force.

(2) Effect of cut spacing on cutting force

Figure 9 shows the relationship curve between average cutting force with groove effects and cut spacing for two types of rocks, which has been subjected to regression analysis as well. As cut spacing increases, there is an increasing trend in average cutting force for both types of rocks. Rhyolite clastic rocks generally has a larger average cutting force than carbonaceous slate specimens at any given cut spacing

(3) Effect of ratio of cut spacing to cut depth on cutting force

Figure 10 shows the relationship curve between average cutting force with groove effects and ratio of cut spacing to cut depth for two types of rocks, which has also been subjected to regression analysis. It can be seen that there is a strong linear relationship between cutting force and the ratio of cut spacing to cut depth. As the ratio increases, there is an increasing trend in average cutting force for both types of rocks, but the growth rate is small. Rhyolite clastic rocks generally has a higher average cutting force than carbonaceous slate specimens at any given ratio.

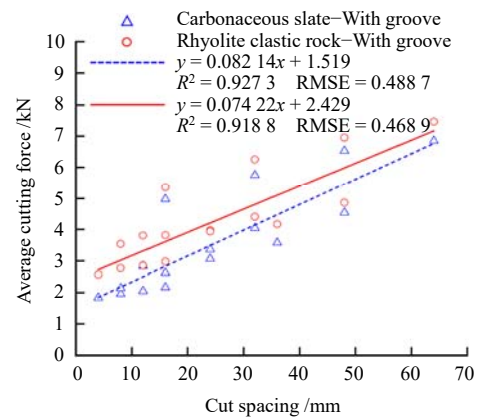


Fig. 9 Diagrams of average cutting force versus cutting spacing

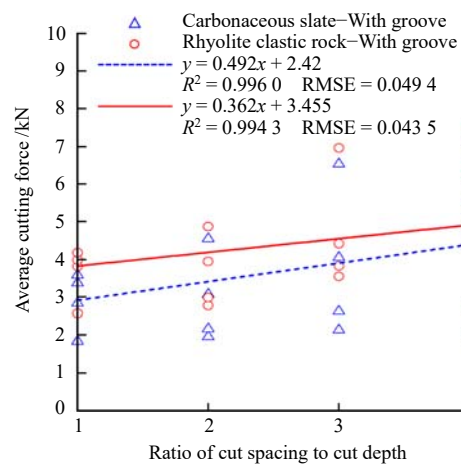


Fig. 10 Diagrams of average cutting force versus the ratio of cutting spacing to cut depth

2.4.3 Specific cutting energy

(1) Effect of cut depth on specific cutting energy

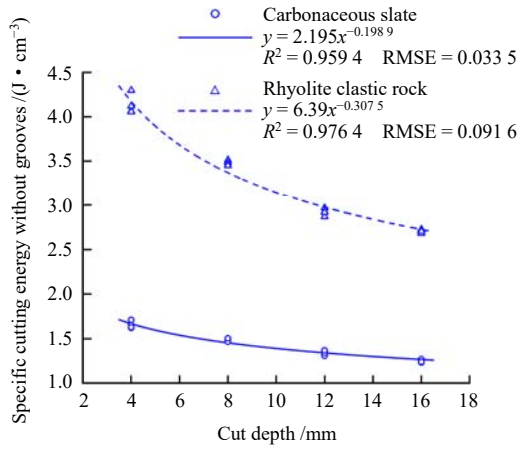
Figure 11 shows the regression analysis of the relationship between specific cutting energy and cut depth for carbonaceous slate and rhyolite clastic rock. It is found that there is a strong linear relationship. The specific cutting energy without groove effects and the optimal specific cutting energy (i.e., minimum specific cutting energy) with groove effects of carbonaceous slate are both lower than that of rhyolite clastic rock. As the cut depth increases, the specific cutting energy without groove effects and the optimal specific cutting energy decrease exponentially, and the optimal specific cutting energy is significantly lower than the specific cutting energy without groove effects, and the remaining specific cutting energy with groove effects are evenly distributed between them, showing a decreasing trend as cut depth increases. Compared to the specific cutting energy without groove effects, carbonaceous slate has a 27.43%–47.91% reduction in specific cutting energy with groove effects, while rhyolite clastic rock has a 25.38%–46.48% reduction.

(2) Effect of the ratio of cut spacing to cut depth on

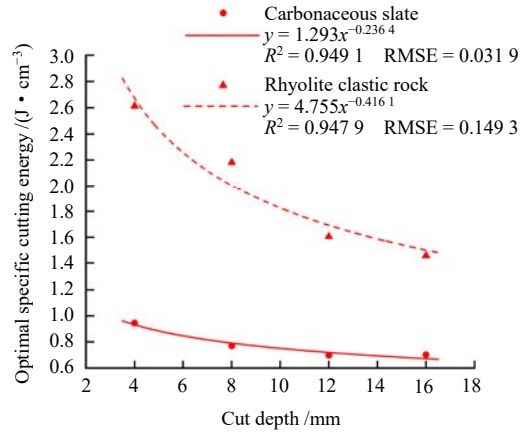
specific cutting energy

Figures 12 and 13 depict the relationship between the specific cutting energy and the ratio of cut spacing to cut depth for carbonaceous slate and rhyolite clastic

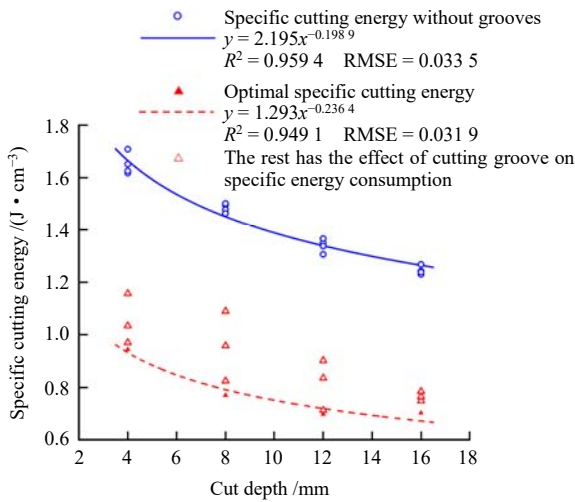
rock during the second cutting. For a given cut depth, a larger specific cutting energy is observed when the ratio is 1 and 4, while a smaller value is observed under the ratio of 2 and 3. As the ratio increases, the specific cutting



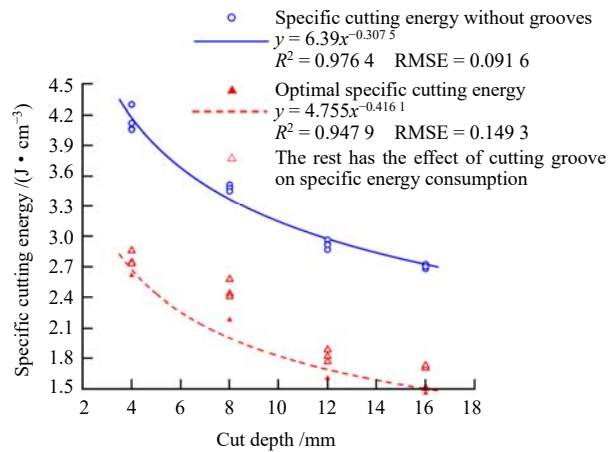
(a) Relationship between specific cutting energy without groove effects and cut depth



(b) Relationship between optimal specific cutting energy and cut depth



(c) Relationship between specific cutting energy of carbonaceous slate and cut depth



(d) Relationship between specific cutting energy of rhyolite clastic rock and cut depth

Fig. 11 Relationship between specific cutting energy and cutting depth

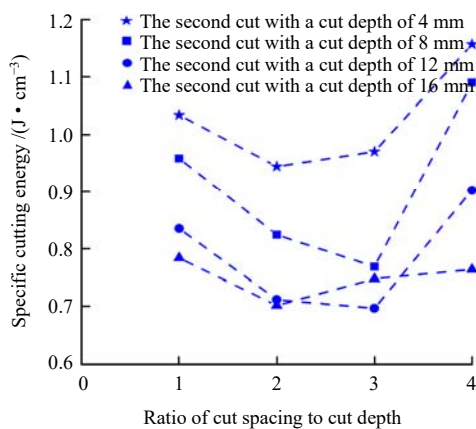


Fig. 12 Relationship between specific cutting energy of carbonaceous slate and the ratio of cut spacing to cutting depth

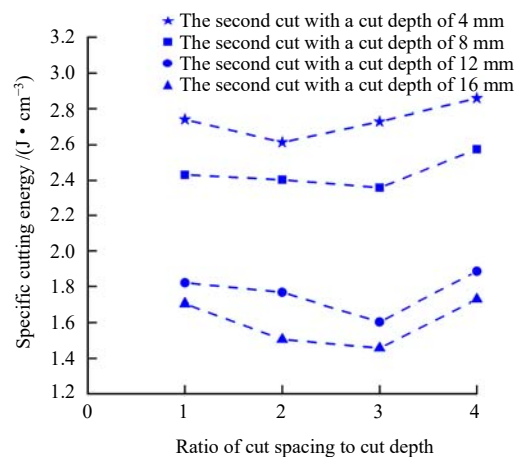


Fig. 13 Relationship between specific cutting energy of rhyolite clastic rock and the ratio of cut spacing to cutting depth

energy initially decreases and then increases in a similar way, regardless of experimental conditions, and there exists a minimum specific cutting energy. This indicates a transition from over-cutting and connected cracks to non-connected cracks. The results also show that there exists an optimal value of 2 or 3 that minimizes the specific cutting energy for different cut depths. Moreover, rhyolite clastic rock exhibits a higher specific cutting energy than carbonaceous slate after the second cut, indicating that a higher strength gives rise to a larger specific cutting energy, which makes rock more difficult to be cut.

Based on experimental data from carbonaceous slate and rhyolite clastic rock, Figure 14 presents a linear relationship between the optimal specific cutting energy and the specific cutting energy without groove effects. The optimal specific cutting energy is approximately 43.5% lower than specific cutting energy without groove effects. The regression equation has a high coefficient of determination ($R^2 = 0.9854$) and small root-mean-square error (RMSE = 0.0952), indicating good model performance.

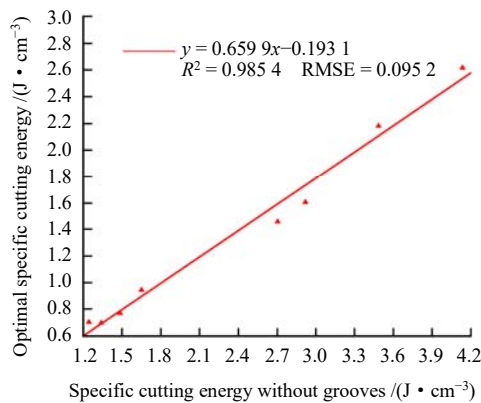


Fig. 14 Relationship between optimal specific cutting energy and specific cutting energy without grooves

3 Field application

3.1 Optimization design of cutting head for roadheader

Figure 15 shows the overall view of the selected SCR260 cantilever roadheader in this study.

The cutting head is the working mechanism of the roadheader. It uses pick arranged in a certain pattern on the cutting head to cut rocks. The rock-breaking performance of the cutting head directly affects the excavation efficiency and service life of the roadheader. The design of the cutting head should not only consider mechanical strength and external dimensions, but also the arrangement of pick, which is closely related to the cutting pattern and rock-breaking mechanism of the cutting head.

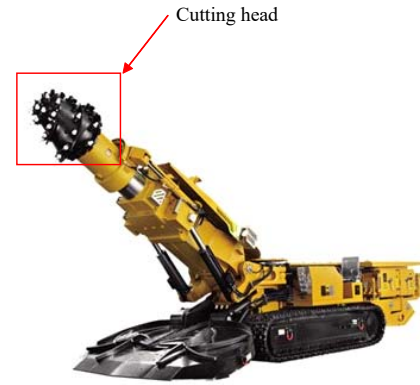


Fig. 15 Full view of SCR260 cantilever roadheader

For carbonaceous slate and rhyolite clastic rock, the average cut depth of the pick on the cutting head is determined to be 10 mm by combining previous research results^[28] and similar excavation practices for similar strong surrounding rocks. According to the conclusions of the aforementioned laboratory experiments, the specific cutting energy is minimized and rock-breaking effect is optimized when the axial spacing between two adjacent picks, i.e., cut distance, is 2–3 times the cut depth. Therefore, it can be inferred that maximum cut spacing should not exceed 30 mm. The picks on the cutting head are divided into three areas (Fig. 16): cone area or main cutting area where swinging motion is mainly used for rock breaking, and the cut spacing should be determined based on the cut experimental results or experience; transitional area or rounded area where both drilling and swinging motions are used, and a smaller cut distance is better since the larger inclination angle and poor conditions; end area or drilling area where drilling motion dominates with very large inclination angle up to 90°, and minimal swinging motion requires even smaller cut distance to reduce transverse swing of cut teeth.

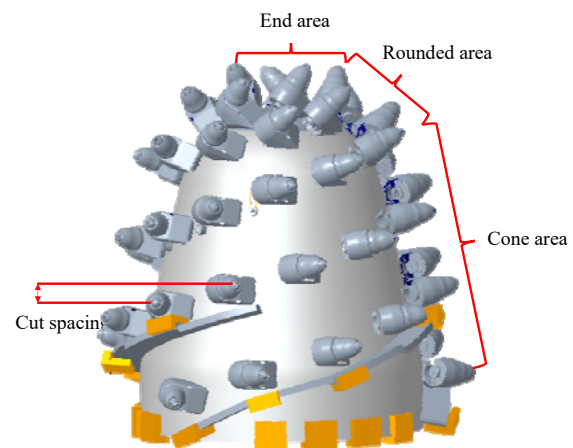


Fig. 16 3D model of a cutting head

According to the aforementioned principle, a total of

49 picks are arranged on the cutting head. The picks are same as that used in laboratory tests, with a cutting angle of 54°. The picks are arranged on three helical lines on the cutting head, and each helical line has a similar trajectory, numbered sequentially from the cone zone to the end zone. The arrangement and distribution of the picks on the three helical lines are shown in Fig. 17, where S represents the cut spacing and S_n represents the groove spacing. The difference in circumferential angle between two adjacent picks is the cutting angle. The circumferential spacing angle C_s on the same helical line is determined as 30°, and the average nearest circumferential spacing angle C_n is 10°. The cone angle of the conical part is 26° (13° per side), and $C_s/C_n = 3$. The serial numbers of picks on the three helical lines are 1-4-7-10-13-16-19-22-25-28-31-34-37-40-43-46-49, 2-5-8-11-14-17-20-23-26-29-32-35-38-41-44-47 and 3-6-9-12-15-18-21-24-27-30-33-36-39-42-45-48, respectively.

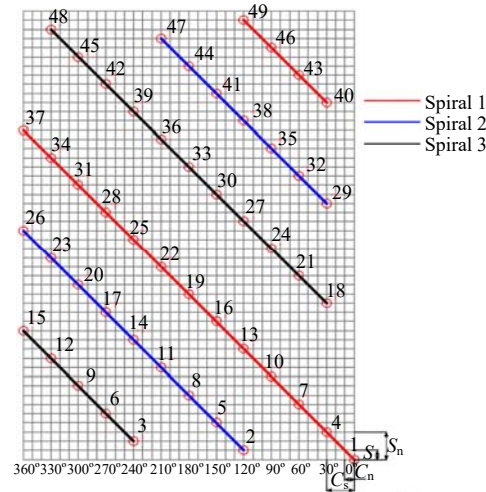
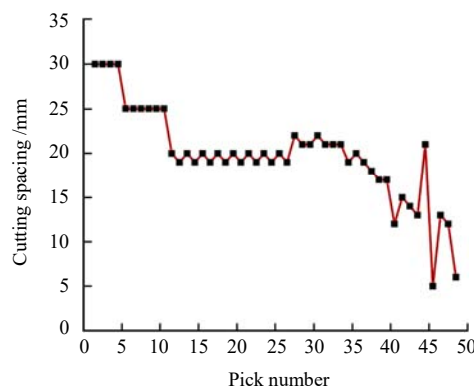


Fig. 17 Pick arrangement

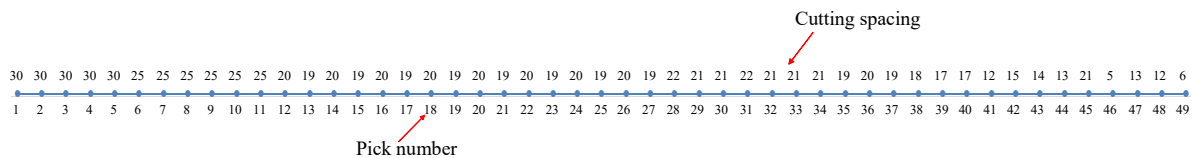
The number and cut spacing of picks in all areas of the cutting head are listed in Table 4. Figure 18 shows

Table 4 Pick number and cut spacing statistics for each division of the cutting head

Cone area											
Adjacent picks	1-2	2-3	3-4	4-5	5-6	6-7	7-8	8-9	9-10	10-11	11-12
Cutting spacing /mm	30	30	30	30	25	25	25	25	25	25	20
Adjacent picks	12-13	13-14	14-15	15-16	16-17	17-18	18-19	19-20	20-21	21-22	22-23
Cutting spacing /mm	19	20	19	20	19	20	19	20	19	20	19
Adjacent picks	23-24	24-25	25-26	26-27	27-28	28-29	29-30				
Cutting spacing /mm	20	19	20	19	22	21	21				
Rounded area											
Adjacent picks	30-31	31-32	32-33	33-34	34-35	35-36	36-37	37-38	38-39	39-40	40-41
Cutting spacing /mm	22	21	21	21	19	20	19	18	17	17	12
Adjacent picks	41-42	42-43	43-44	44-45							
Cutting spacing /mm	15	14	13	21							
End area											
Adjacent picks	45-46	46-47	47-48	48-49							
Cutting spacing /mm	5	13	12	6							



(a) Line graph of cut spacing and pick number



(b) Schematic diagram of cut spacing and pick number

Fig. 18 Relationship between cut spacing and pick number

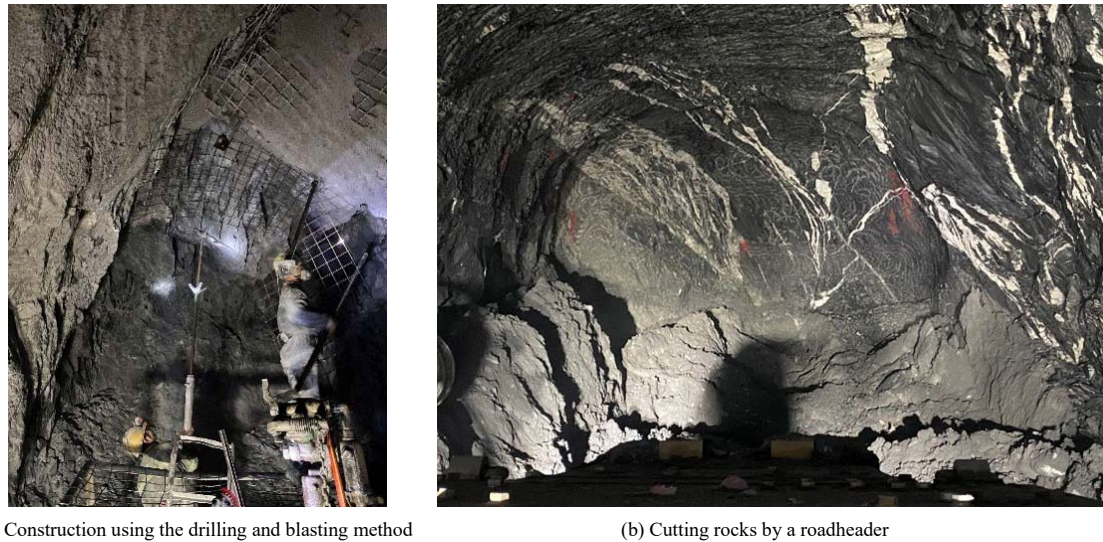


Fig. 19 Comparison of roadway excavation sections

the relationship between cut spacing and pick number. Pick numbered from 1 to 29 belong to the cone area, 30 to 44 the rounded area, and 45 to 49 the end area. Due to the specific external structure of the cutting head transitioning from the rounded area to the end area, increasing the cut spacing of the transitional section to some extent can reduce the external force acting on teeth 44 and 45, making it easier to balance drilling and swing cutting and prolonging the service life of adjacent picks.

3.2 Field test verification

Starting from March 1st, 2021, non-explosive excavation industrial tests using a cantilevered roadheader were conducted in 3 780 m level section of roadway at a silver-polymetallic mine in Sichuan Province. Surrounding rocks mainly consists of carbonaceous slate and rhyolite clastic rocks. The size of roadway is 3.5 m×3.5 m with a cross-section area of 11.38 m². Figure 19 shows a comparison of the excavated roadway sections, which indicates that compared to drilling and blasting methods, the roadway section cut by the roadheader has better forming quality, controllable overbreak/underbreak, and less damage to

surrounding rocks.

For this high-altitude and cold mine, a comparison of the main technical and economic indicators between the drilling and blasting method and the roadheader cutting method before and after improving picks is listed in Table 5. It can be seen that compared to the traditional drilling and blasting method, the cutting efficiency using roadheader significantly was raised after improving picks and overall excavation costs were reduced. Compared to cutting without improvement in picks, both single footage and daily footage were significantly increased, and cutting energy consumption, consumption of pick and total cost of excavation were greatly reduced. These indicators demonstrate that optimizing the pick layout scheme is reasonable as it reduces load fluctuations on cutting heads and balances their lifespan to improve the cutting performance of roadheader. This approach utilizes appropriate cutting heads of roadheader to match hard rocks, which plays an extremely important role in improving economic efficiency for hard rock tunnel excavation.

Table 5 Comparison of main technical and economic indexes of the drilling and blasting method and roadheader cutting

Construction methods	Single footage /m	Number of daily cycles /times	Daily footage /m	Pure cutting time per day /h	Daily volume of rock excavated /m ³	Energy consumption for cutting /(kW · h · m ⁻³)	Consumption of picks /(pcs · m ⁻¹)	Total cost of excavation /(yuan · m ⁻³)
Traditional drilling and blasting method	2.51	1	2.51	—	28.56	—	—	652.2
Roadheader cutting before improving picks	0.57	6	3.42	6.3	38.92	41.76	0.84	368.1
Roadheader cutting after improving picks	0.68	6	4.08	6.1	46.43	33.24	0.58	247.5

4 Conclusions

(1) Using the TRW-3000 true triaxial electro-hydraulic

servo testing system and an innovative pick loading platform, indoor linear cutting tests were conducted on carbonaceous slate and rhyolite clastic rock specimens to explore the

failure modes of rock breaking by picks and study the effects of different cut depths and cut spacings on cutting force and specific cutting energy. The results indicate that there are four failure modes for rock breaking, and there is a significant synergistic effect between two adjacent picks. The average cutting force increases linearly with the increase in both cut depth and cut spacing. Both the specific cutting energy with and without groove impact decrease exponentially with increasing cut depth. The specific cutting energy decreases first, and then increases with the increase in the ratio of cut spacing to cut depth. This variation trend is insensitive to experimental conditions. There is an optimal range (2–3) of the ratio that produces the best rock breaking effect with minimum specific cutting energy, which represents a transition from overcutting and optimal cutting to undercutting. Under the same experimental conditions, carbonaceous slate specimens have a lower specific cutting energy than rhyolite clastic rocks, indicating a positive correlation between specific cutting energy and rock strength.

(2) Based on the conclusions of laboratory experiments, optimization design was carried out on the arrangements of 49 picks in the conical, rounded and end areas of the cutting head of cantilevered roadheader. They were arranged in three spiral lines with a line spacing designed to be 2–3 times the cut depth for swing-cutting rock breaking in the conical area. A relatively smaller cut spacing was designed for the rounded area which considers both drilling and swing-cutting, and an even smaller cut spacing for the end area which mainly uses drilling method for rock breaking. Industrial tests were carried out on non-explosive excavation of a silver-polymetallic mine in Sichuan. The tests proved that compared with the drilling and blasting method, the roadheader cutting by using improved pick arrangement achieved fully mechanized, safe, efficient, low-cost and non-blasting continuous excavation. Compared with the cutting results before improvement, the roadheader with improved pick arrangement significantly enhanced excavation efficiency and reduced the overall cost, which achieves prominent success and can provide reference for similar mining and excavation activities.

References

- [1] OCAK I, BILGIN N. Comparative studies on the performance of a roadheader, impact hammer and drilling and blasting method in the excavation of metro station tunnels in Istanbul[J]. *Tunnelling and Underground Space Technology*, 2010, 25(2): 181–187.
- [2] HEKIMOGLU, ZEKI O. Investigations into tilt angles and order of cutting sequences for cutting head design of roadheaders[J]. *Tunnelling and Underground Space Technology*, 2018, 76: 160–171.
- [3] MA Hong-su, GONG Qiu-ming, WANG Ju, et al. Study on the influence of confining stress on TBM performance in granite rock by linear cutting test[J]. *Tunnelling and Underground Space Technology*, 2016, 57: 145–150.
- [4] LI Xi-bing, YAO Jin-rui, DU Kun. Preliminary study for induced fracture and non-explosive continuous mining in high-geostress hard rock mine—a case study of Kaiyang phosphate mine[J]. *Chinese Journal of Rock Mechanics and Engineering*, 2013, 32(6): 1101–1111.
- [5] LI Xi-bing, ZHOU Jian, WANG Shao-feng, et al. Review and practice of deep mining for solid mineral resources[J]. *The Chinese Journal of Nonferrous Metals*, 2017, 27(6): 1236–1262.
- [6] LI Xi-bing, HUANG Lin-qi, ZHOU Jian, et al. Review and practice of deep mining for solid mineral resources[J]. *The Chinese Journal of Nonferrous Metals*, 2019, 29(9): 1828–1847.
- [7] LI Xi-bing, LIU Zhi-xiang, PENG Kang, et al. Theory and practice of rock mechanics related to the exploitation of under seam metal mine[J]. *Chinese Journal of Rock Mechanics and Engineering*, 2010, 29(10): 1945–1953.
- [8] DU Kun, TAO Ming, LI Xi-bing, et al. Experimental study of slabbing and rock burst induced by true-triaxial unloading and local dynamic disturbance[J]. *Rock Mechanics and Rock Engineering*, 2016, 49(9): 3437–3453.
- [9] LIU Wei-ji, ZHU Xiao-hua, JING Jun. The analysis of ductile-brittle failure mode transition in rock cutting[J]. *Journal of Petroleum Science & Engineering*, 2018, 163: 311–319.
- [10] ZHANG Meng-qi. Influence of pick array circumferential angle on cutting performance of longitudinal cutting head[J]. *Colliery Mechanical & Electrical Technology*, 2013(2): 19–23.
- [11] YURDAKUL M, GOPALAKRISHNAN K, AKDAS H. Prediction of specific cutting energy in natural stone cutting processes using the neuro-fuzzy methodology[J]. *International Journal of Rock Mechanics and Mining Sciences*, 2014, 67(67): 127–135.
- [12] YILMAZ N G, TUMAC D, GOKTAN R M. Rock cuttability assessment using the concept of hybrid dynamic hardness (HDH)[J]. *Bulletin of Engineering Geology & the Environment*, 2015, 74(4): 1363–1374.
- [13] LJY A, QMG B, JZ A. Study on rock mass boreability by TBM penetration test under different in situ stress conditions[J]. *Tunnelling and Underground Space Technology*,

- 2014, 43: 413–425.
- [14] GUNES N, YURDAKUL M, GOKTAN R M. Prediction of radial bit cutting force in high-strength rocks using multiple linear regression analysis[J]. *International Journal of Rock Mechanics and Mining Sciences*, 2007, 44(6): 962–970.
- [15] BALCI C, DEMIRCIN M A, COPUR H, et al. Estimation of optimum specific energy based on rock properties for assessment of roadheader performance (567BK)[J]. *Journal-South African Institute of Mining and Metallurgy*, 2004, 104(11): 633–642.
- [16] TIRYAKI B, DIKMEN A C. Effects of rock properties on specific cutting energy in linear cutting of sandstones by picks[J]. *Rock Mechanics and Rock Engineering*, 2006, 39(2): 89–120.
- [17] WANG Shao-feng, SUN Li-cheng, LI Xi-bing, et al. Experimental investigation and theoretical analysis of indentations on cuboid hard rock using a conical pick under uniaxial lateral stress[J]. *Geomechanics and Geophysics for Geo-Energy and Geo-Resources*, 2022, 8(1): 1–23.
- [18] ZHANG Zong-xian, OUCHTERLONY F. Energy requirement for rock breakage in laboratory experiments and engineering operations: a review[J]. *Rock Mechanics and Rock Engineering*, 2022, 55: 629–667.
- [19] WANG Xiang, LIANG Yun-pei, WANG Qing-feng, et al. Empirical models for tool forces prediction of drag-typed picks based on principal component regression and ridge regression methods[J]. *Tunnelling & Underground Space Technology*, 2017, 62: 75–95.
- [20] LI Xue-feng. A study on the influence of pick geometry on rock cutting based on full-scale cutting test and simulation[J]. *Advances in Mechanical Engineering*, 2020, 12(12): 1–13.
- [21] LIANG Yun-pei, WANG Xiang, WANG Qing-feng. Effects of cut depth and cut spacing on tool forces acting on a conical pick in rock cutting[J]. *Journal of Vibration and Shock*, 2018, 37(3): 27–33.
- [22] WANG Shao-feng, TANG Yu, LI Xi-bing, et al. Analyses and predictions of rock cuttabilities under different confining stresses and rock properties based on rock indentation tests by conical pick[J]. *Transactions of Nonferrous Metals Society of China*, 2021, 31(6): 1766–1783.
- [23] WANG Shao-feng, LI Xi-bing, DU Kun, et al. Experimental investigation of hard rock fragmentation using a conical pick on true triaxial test apparatus[J]. *Tunnelling and Underground Space Technology*, 2018, 79: 210–223.
- [24] WANG Shao-feng, LI Xi-bing, YAO Jin-rui, et al. Experimental investigation of rock breakage by a conical pick and its application to non-explosive mechanized mining in deep hard rock[J]. *International Journal of Rock Mechanics and Mining Sciences*, 2019, 122: 104063.
- [25] LI Xi-bing, WANG Shao-feng, WANG Shan-yong. Experimental investigation of the influence of confining stress on hard rock fragmentation using a conical pick[J]. *Rock Mechanics and Rock Engineering*, 2017, 51(1): 255–277.
- [26] NUH BILGIN H C, BALCI C. Effect of replacing disc cutters with chisel tools on performance of a TBM in difficult ground conditions[J]. *Tunnelling and Underground Space Technology*, 2012, 27(1): 41–51.
- [27] BILGIN N, DEMIRCIN M A, COPUR H, et al. Dominant rock properties affecting the performance of conical picks and the comparison of some experimental and theoretical results[J]. *Pergamon*, 2006, 43(1): 139–156.
- [28] WANG Xiang. Study on rock breaking mechanism using conical picks and cutting performance of roadheaders[D]. Chongqing: Chongqing University, 2017: 155–165.